Research Square

Preprints are preliminary reports that have not undergone peer review.
They should not be considered conclusive, used to inform clinical practice,
or referenced by the media as validated information.

Intratumoral and Peritumoral Radiomics Based on T2WI and DWI Sequences for predicting microvascular invasion of intrahepatic mass-forming cholangiocarcinoma

Jiamei Ma
Affiliated Hospital of Hebei University
Zhenlong Wang
College of Quality and Technical Supervision of Hebei University
Xiaomeng Li
Affiliated Hospital of Hebei University
Lihong Xing
Affiliated Hospital of Hebei University
Liu Sun
Affiliated Hospital of Hebei University
Shuai Han
Affiliated Hospital of Hebei University
Jinrong Qu
Henan Cancer Hospital
Jinghui Dong
The Fifth Medical Center of Chinese PLA General Hospital
Hongjun Li
Beijing YouAn Hospital
Jlaning Wang
Affiliated Hospital of Hebei University
Kun Liu
College of Quality and Technical Supervision of Hebei University
Xiaoping Yin
hdfyrad@hbu.edu.cn

Affiliated Hospital of Hebei University

Research Article

Keywords: intrahepatic mass-forming cholangiocarcinoma, radiomics, microvascular invasion, magnetic resonance imaging

Posted Date: July 16th, 2026

DOI: https://doi.org/10.21203/rs.3.rs-10169306/v1

License: This work is licensed under a Creative Commons Attribution 4.0 International License.
Read Full License

Additional Declarations: No competing interests reported.

Intratumoral and Peritumoral Radiomics Based on T2WI and DWI Sequences for predicting microvascular invasion of intrahepatic mass-forming cholangiocarcinoma

Jiamei Ma[1,2#], Zhenlong Wang[3#], Xiaomeng Li[1,2], Lihong Xing[1,2], Liu Sun[1,2], Shuai Han[4], Jinrong Qu[4], Jinghui Dong[5], Hongjun Li[6], Jianing Wang[1,2], Kun Liu[4*], Xiaoping Yin[1,2*]

[1]Department of Radiology, Affiliated Hospital of Hebei University, Baoding, People's Republic of China.
[2]Hebei Key Laboratory of Precise Imaging of Inflammation Related Tumors, Baoding, People's Republic of China.
[3]College of Quality and Technical Supervision of Hebei University, Baoding, People's Republic of China;
[4]Department of Radiology, the Affiliated Cancer Hospital of Zhengzhou University & Henan Cancer Hospital, Zhengzhou, People's Republic of China;
[5]Department of Radiology, The Fifth Medical Center of Chinese PLA General Hospital, Beijing, People's Republic of China;
[6]Department of Radiology, Beijing You'an Hospital, Beijing, People's Republic of China.
[#]First authors:
Jiamei Ma, m13785288301@163.com; Zhenlong Wang, dennis.wzl666@gmail.com,These authors contributed equally to this work.
*Corresponding authors:
Xiaoping Yin, hdfyrad@hbu.edu.cn; Kun Liu, liukun15166@hbu.edu.cn,These authors contributed equally to this work.

Ethics approval and consent to participate

The study was conducted in accordance with the Declaration of Helsinki. This retrospective study was approved by the Ethics Committee of Affiliated Hospital of Hebei University(Institutional Review Board approval number：HDFYLL-IIT-2025-121). Written informed consent was waived due to the retrospective nature of the study, as approved by the institutional review board.

Human Ethics and Consent to Participate declarations:

Not applicable.

Availability of data and material :

The data used and analyzed during the current study are available from the corresponding **authors** on reasonable request.

Competing interests

All authors declare that they have no competing interests

Funding

This work was supported by Hebei Province Natural Science Foundation Under Grant H2024201034.

ABSTRACT：

Background: Intrahepatic mass-forming cholangiocarcinoma (IMCC) is the predominant subtype of intrahepatic cholangiocarcinoma (ICC) with poor postoperative prognosis. Microvascular invasion (MVI) is an independent adverse prognostic factor for IMCC, while MVI diagnosis depends on postoperative pathology, and preoperative conventional MRI shows limited diagnostic performance. Existing MVI radiomic prediction models have inherent defects, and relevant peritumoral feature researches are insufficient. Therefore, our primary aim in this study was to construct a combined MRI radiomics model integrating intratumoral, peritumoral imaging features for noninvasive preoperative MVI prediction, and guide individualized treatment for IMCC patients.

Methods： Preoperative MRI scans from IMCC patients were retrospectively obtained from two academic medical centers. Radiomics features were extracted from the intratumoral and multiple peritumoral regions. After feature selection, four machine learning methods were used to establish multiple radiomics models based on different sequences of intratumoral and peritumoral regions. The predictive efficacy of the models was compared and the most effective model was selected. Key variables of clinical imaging features and radiomics were integrated to establish a combined model and its performance was evaluat ed.

Results： The intratumoral and peritumoral 15 mm radiomics model based on the DWI sequence showed the best performance. The area under the receiver operating curves for the training cohort, internal test cohort, and external valida tion cohort were 0.984, 0.826, and 0.735, respectively. The performance of the model was superior to that of the clinical imaging model and the combined model.

Conclusion： The intratumoral + peritumoral 15 mm radiomics model of DWI sequences based on the Random Forest machine learning method showed the best predictive ability. The ability of the model to predict IMCC MVI noninva sively before surgery makes it a valuable tool for providing theoretical guidance for clinical treatment decision-making.

Keywords: intrahepatic mass-forming cholangiocarcinoma; radiomics; microvascular invasion; magnetic resonance imaging.

Introduction

Intrahepatic cholangiocarcinoma (ICC), which originates from the intrahepatic bile duct epithelium, is the second most common primary liver malignancy[1]. The morbidity and mortality of ICC have increased globally in recent years[2,3]. Intrahepatic mass-forming cholangiocarcinoma (IMCC) is the most common subtype of ICC, accounting for approximately 60% of cases [4]. The prognosis of patients with this type of tumor is extremely poor, and the 5-year overall survival rate after surgery is 20%-40%[5]. Microvascular invasion (MVI) is

defined as the presence of cancer cell nests in the lumen of organs lined with endothelial cells, as detected under a microscope[6]. Positive MVI is considered an independent risk factor for early recurrence, intrahepatic metastasis, and shorter overall survival in patients with ICC after surgery[7-10]. However, the current gold standard for the diagnosis of MVI is based on pathological examination of resected specimens, which limits clinical decision-making. Magnetic resonance imaging (MRI) plays a key role in the preoperative evaluat ion of ICC[11]. However, radiologists rely on subjective morphological signs to indirectly determine MVIstatus, and their diagnostic efficacy is thus limited by low sensitivity, differences in specificity, and large differences between observer s.

Artificial intelligence-based prediction of the tumor microenvironment has become a research hotspot in recent years. Radiomics extracts quantitative features from medical images using high-throughput computer software. Radiomics features are then screened using statistics and machine learning and combined with clinical, conventional radiation, and other radiomics features to construct a prediction model for disease diagnosis, treatment response, and prognosis[12-14]. Radiomics is used widely in ICC research, and prediction models for IMCC MVI have emerged in recent years. However, current research results are variable, and most studies are based on small sample sizes and a single-center retrospective design, in addition to being limited to the extraction of radiomic features from IMCC tumors[15-16].MVI usually appears inthe area surrounding the tumor.The peritumoral area refers to the transition zone between tumor lesions and normal tissues. The microenvironment of this area has unique physical and immune characteristics and is involved in the processes related to tumorigenesis and tumor development. Radiomic features extracted from the peritumoral area are important for predicting tumor MVI[17]. There are currently few studies addressing the prediction of IMCC MVI based on different peritumoral regions. In this study, we developed a combined prediction model based on intratumoral and peritumoral MRI radiomics features and clinical imaging features. This model is expected to achieve non-invasive prediction of IMCC MVI before surgery and provide theoretical guidance for the design of individualized treatment strategies for patients.

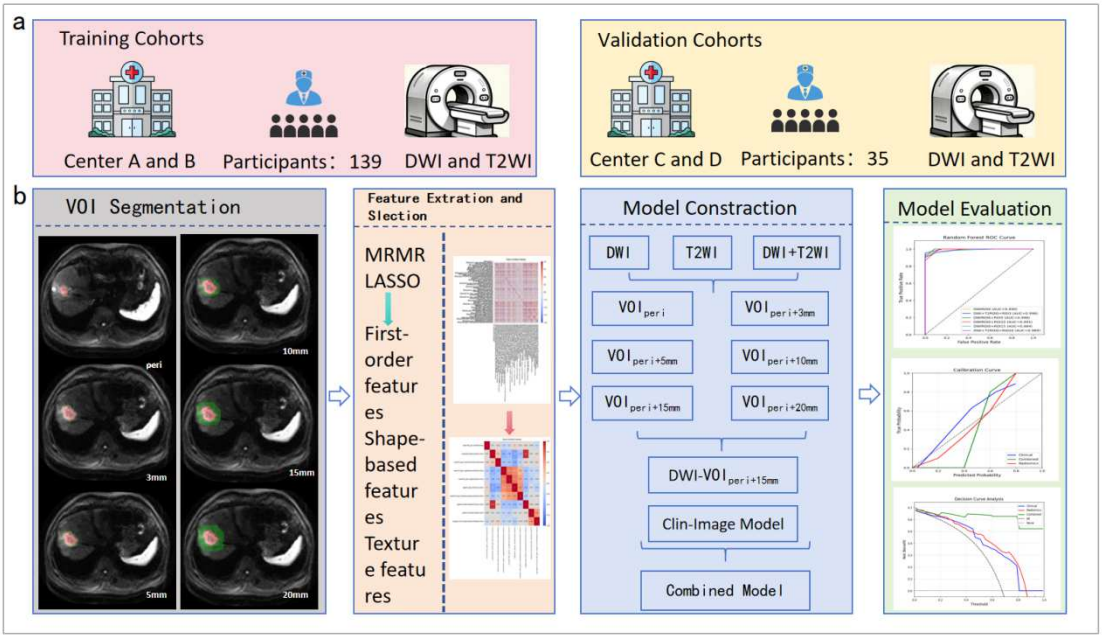


Figure 1 | Overview of the study design. (a) The datasets for training were obtained from two distinct medical c-enters, while the datasets for independent validation were procured from a medical center located in a different area. (b) Radiomics framework of distinguishing intrahepatic massforming cholangiocarcinoma from liver metastasis, Ev-aluate and compare the diagnostic performance of the clinical-image model, radiomics model, and combined model.VOI, volume of interest; VOIperi, VOI peripheral.

Materials

This study used a multi-center retrospective design. Clinical and preoperative MRI data of 276 patients with IMCC confirmed by surgery and pathology from two medical institutions between January 2018 and July 2024 were collected. Data from 51 IMCC patients treated during the same period in two medical institutions were also collected as an external test cohort. The inclusion criteria were as follows: patients with a single lesion histologically confirmed as IMCC; patients who underwent liver MRI examination [including T2WI-weighted imaging (T2WI), and diffusion-weighted imaging (DWI)] within 1 month before surgery; patients who did not receive any previous treatment for liver lesions or primary colorectal lesions. The exclusion criteria were as follows: other types of ICC (such as ICC with periductal infiltration or intraductal growth pattern); missing preoperative MRI data or data collected outside the specified time period;poor quality of MRI images due to severe artifacts or noise. The demographic and clinical data of the patients were obtained from the electronic medical record system. This retrospective study was approved by the institutional review board (HDFYLL-IIT-2025-121) and exempted from the need for informed consent from patients. The overall research process is shown in Figure 2. This studystrictly followed the Checklist for Evaluation of Radiomics research guidelines.

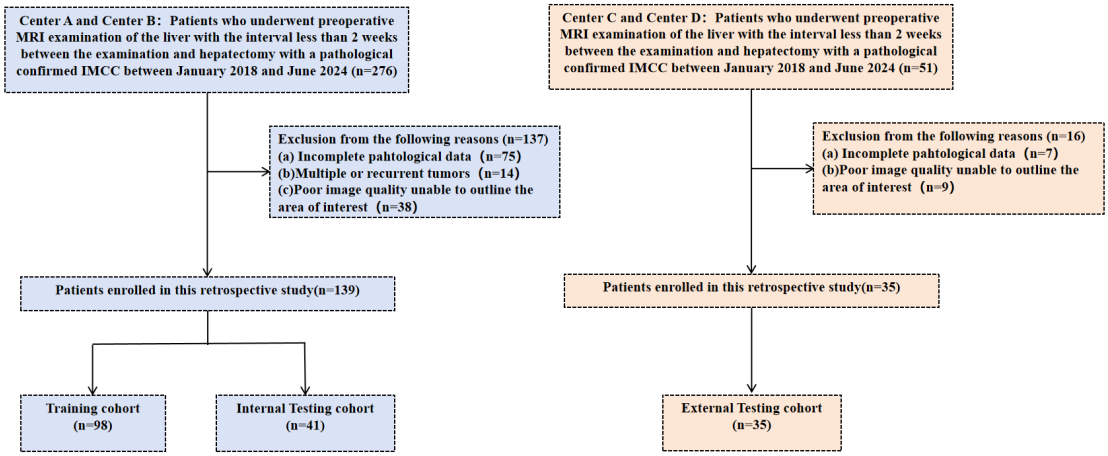


Figure 2 | Flowchart of the patient inclusion and exclusion process. IMCC, intrahepatic mass-forming cholangiocarcinoma.

MRI image acquisition and preprocessing

Preoperative abdominal MRI was performed using one of the following MRI scanners: Discovery MR 750 3.0T (GE Healthcare, Milwaukee, WI, USA), uM R 588 1.5T (United Imaging, Shanghai, China), or Signa HDx 3.0T (GE Healt hcare, Milwaukee, WI, USA). The Siemens Amira 1.5T MRI scanner (German y)and the Philips Achieva 1.5T MRI scanner (The Netherlands) liver examinati onprogram included axial T2WI, and DWI(specific scanning parameters are sho wnin the attached table S1). DWI was performed using respiratory triggering o r

diaphragm navigation techniques, combined with axial single-shot spin echo and echo-planar imaging sequences, as well as diffusion-weighted gradients applied in three orthogonal directions (b-values of 0 and 800 s/mm).The sitkBSpline interpolation algorithm in the SimpleITK library was used to resample each im age to ensure that the resolution of all images was 1 × 1 × 1 mm. This was necessary to eliminate the influence of different scanning resolutions and provid e standardized data for subsequent feature extraction.

MRI analysis

Two radiologists evaluated preoperative multi-parameter MRI scans. Radiologist 1 had 5 years of experience in abdominal radiology and radiologist 2 had 6 y ears of experience in the field. In cases of disagreement between the two doct ors, a third senior radiologist (radiologist 3) with 20 years of experience in ab dominal radiology was consulted. In the end, the three radiologists came to an agreement after a thorough discussion. The three radiologists were blinded to t he patients' clinical data and pathological results. Tumor thrombus refers to the growth or extension of the tumor to adjacent blood vessels. The vascular penet ration sign describes the extension of blood vessels into the tumor. Lymphaden opathy is characterized by a short axis diameter of 1 cm or more. MRI manif estations were described according to the following parameters: lesion location (left lobe of the liver, right lobe of the liver, or both), tumor margin (smooth

or infiltrative), T2WI tumor boundary (clear or blurry), bile duct dilatation (pre sent or absent), hepatic capsule retraction (present or absent), intrahepatic bile duct stones (present or absent), tumor thrombus (present or absent), vascular traversal sign (present or absent), enlarged lymph nodes (present or absent), T2WI signal (homogeneous high signal, inhomogeneous high signal, low signal, peripheral high signal internal low signal, peripheral low signal internal high signal, or equal signal)[18,19]; and DWI signal (uniform high signal, uneven high signal, peripheral high signal, or internal low signal)[18,19].

Radiomics analysis

Tumor segmentation and extension

All image data were obtained from the picture archiving and communication system (PACS). The data were stored in DICOM format by two radiologists (attending physician with 5 years of experience and deputy chief physician with 10years of experience) blinded to the pathological results and clinical data. The software ITK-SNAP (v.3.8.0) was used to delineate the IMCC lesion area layer by layer on DWI, and T2WI sequences to obtain the region of interest (VOI) of the tumor. If the VOI delineation was controversial, the two doctors reachedan agreement through discussion. The Nibabel 5.3.0 algorithm package (https://github.com/nipy/nibabel/releases/tag/5.3.0), NumPy 1.6.4 algorithm packag e (https://pypi.org/project/numpy/1.26.4/ # files) and SciPy algorithm package (h ttps://pypi.org/project/scipy/1.13.1/) in the Python library were used to extend th e delineated VOI outwards by 3, 5, 10, 15, and 20 mm to obtain the peritumo ral andtumor + peritumoral areas. When VOI was extended, the surrounding large blood vessels and bile ducts were avoided as much as possible, and the volume beyond the liver contour was manually removed by two radiologists. In traclass correlation coefficient (ICC) was used to evaluate intraobserver and int erobserver reliability.

Radiomics feature extraction and screening

Python-based PyRadiomics (v. 3.0.1) was used for image preprocessing and feature extraction, followed by feature screening using Least Absolute Shrinkage and Selection Operator (LASSO) regression and the Maximum Correl ation Minimum Redundancy (MRMR) algorithm. The LASSO regression algorithm wasused for feature selection. L1 regularization was used to compress feature coefficients, and unimportant feature coefficients were compres sed to zero. GridSearchCV 5-fold cross-validation was used, and the evaluationi ndex was negative mean square error. The regularization parameter alpha of L ASSO was optimized to improve the accuracy of feature selection. The MRMR algorithm was used to minimize the redundancy between features while maxi mizing the correlation between features and labels. The K value of MRMR wa s dynamically adjusted according to the feature redundancy of the data to enab le the algorithm to adapt to different data characteristics. This adaptive method enhances the robustness and applicability of the algorithm.

Model building and validation

In this study, we used four classifiers: Random Forest, Logistic Regression, XGBoost, and Gaussian Naive Bayes to establish the model. The training cohort to internal validation cohort ratio was 7: 3. To ensure the fairness and accuracy of the model evaluation, we used five-fold cross-validation. This method keeps the proportion of each category sample consistent with the original data cohort in each compromise. The results of each fold-validation were combined to yield the data for the final evaluation and analysis. The established models included DWI, T2WI intratumoral radiomics model, DWI, T2WI intratumoral + peritumoral radiomics model, and combined model, and the best model was selected. Firstly, we constructed 72 candidate models (4 machine learning methods× 3 sequences × 6 VOIs: 0/ 3/ 5/ 10/ 15/ 20 mm). The area under the receiver operating curve (AUC) and the parameters of accuracy, sensitivity, specificity, positive predictive rate, and negative predictive rate were used to analyze the classifier, as shown in table S2. After selecting the best classifier, themost effective model for each VOI was selected, and the pairwise DeLong test was used to determine the optimal peritumoral model.

For the clinical-imaging model, univariate logistic regression analysis was performed to evaluate the differences in clinical and imaging features between IMCC MVI positive and negative patients in the training cohort. Variables with a pvalue <0.05 were considered statistically significant and used to construct a clinical-imaging model. Finally, we combined the radiomics model with the clinical imaging model to construct the final combined model.

Statistical analysis

Statistical analysis was performed using Python (v. 1.26.4) and SPSS software (v. 26.0). In the comparison of clinical features and imaging features, continuous variables were tested using the one-way variance F test, and categorical variables were tested using the chi-square test or Fisher's exact test. They were used to compare the characteristics of patients in the training cohort, internal testcohort, and external test cohort, and to compare the characteristics of MVI-positive and -negative patients in each group. Univariate logistic regression analysiswas used to evaluate the differences in clinical and imaging characteristics between MVI-negative and -positive patients, and the characteristics with p <0.05 were selected as the characteristics of the clinical-imaging model. The clinical-imaging model was created using the random forest algorithm; the training cohort and internal test cohort were divided at a ratio of 7: 3, and 5-fold cross-validation was performed. A ROC curve was drawn to analyze and evaluate the predictive performance of the model, and the following performance indicators were calculated: accuracy, F1-score, sensitivity, specificity, positive predictive rate, and negative predictive rate. The diagnostic performance of the different models was compared using the DeLong test,and the statistical significance of thetwo-sided test was set to p <0.05. The consistency and clinical value of the model were evaluated using a calibration curve and decision curve analysis (DCA).

Results

Baseline characteristics and clinical imaging model construction

According to the inclusion criteria, 139 IMCC patients (91 men and 48 women) were finally included in the study. Among them, 97 patients with an average a ge of 39.938 ± 19.000 years were classified as the training group and 42 patie nts with an average age of 45.381 ± 20.131 years were classified as the test g roup. Another 35 patients served as the external validation cohort (Table 1 su mmarizes the comparative results of demographic, clinical, and radiological char acteristics). Univariate logistic regression analysis identified age, T2WI signal, a nd DWI signal as independent predictors of IMCC pathological grade (Table 2);

these variables were included in the clinical imaging model. The AUC of the model in the training cohort, internal test cohort, and external validation cohort were 0.813, 0.819 and 0.663, respectively.

Table 1 Patient and imaging characteristics in the training cohort ， Internal testing cohort and external cohort.

Characteristic	**Training cohort (n=97)**	**Internal validation cohort (n=42)**	**External validation cohort (n=35)**	**χ^2/F**	***P***
Age (year)	39.938±19.000	45.381±20.131	50.200±15.573	4.230①	0.016*
Sex					
Male	60(61.860%)	31(73.810%)	21(60.000%)	2.190②	0.334
Female	37(38.140%)	11(26.190%)	14(40.000%)		
Lesion Location					
Left Lobe	41(42.270%)	21(50.000%)	17(48.570%)	2.042②	0.728
Right Lobe	44(45.360%)	15(35.710%)	12(34.290%)		
Both	12(12.370%)	6(14.290%)	6(17.140%)		
Tumor margin					
Smooth	47(48.450%)	20(47.620%)	31(88.570%)	15.661②	0.000***
Infiltrative	50(51.550%)	22(52.380%)	4(11.430%)		
T2WI tumor boundary	54(55.670%)	26(61.900%)	24(68.570%)	8.106②	0.017*
Clear					
Blurry	43(44.330%)	16(38.100%)	11(31.430%)		
Bile duct Dilatation				0.073②	0.964
Yes	41(42.270%)	17(40.480%)	14(40.000%)		
No	56(57.730%)	25(59.520%)	21(60.000%)		
Hepatic capsule retraction				2.896②	0.235
Yes	43(44.330%)	16(38.100%)	20(57.140%)		
No	54(55.670%)	26(61.900%)	15(42.860%)		
Intrahepatic bile duct stones				1.317③	0.571
Yes	2(2.060%)	2(4.760%)	2(5.710%)		
No	95(97.940%)	40(95.240%)	33(94.290%)		
Vascular involvement				18.792②	0.002**
Yes	37(38.140%)	10(23.810%)	25(71.430%)		
No	60(61.860%)	32(76.190%)	10(28.570%)		
Vascular traversal Sign	35(36.080%)	8(19.050%)	20(57.140%)	11.997②	0.002**
Yes	62(63.920%)	34(80.950%)	15(42.860%)		

Characteristic	Training cohort (n=97)	Internal validation cohort (n=42)	External validation cohort (n=35)	χ^2/F	*P*
No					
Suspicious lymph nodes					
Yes	17(17.530%)	6(14.290%)	23(46.940%)	28.106②	0.000***
No	80(82.470%)	36(85.710%)	26(53.060%)		
T2WI signal					
Pattern					
homogeneous high signal	28(28.870%)	9(21.430%)	3(8.570%)		
inhomogeneous high signal	51(52.580%)	25(59.520%)	29(82.860%)		
low signal peripheral high signal internal low signal	0(0.000%)	2(4.760%)	0(0.000%)	10.716②	0.098
peripheral low signal internal high signal equal signal	8(8.250%)	2(4.760%)	1(2.860%)		
	6(6.190%)	2(4.760%)	2(5.710%)		
	4(4.120%)	2(4.760%)	0(0.000%)		
DWI signal					
Pattern					
homogeneous high signal	30(30.930%)	9(21.430%)	2(5.710%)		
inhomogeneous high signal	48(49.480%)	25(59.520%)	26(74.290%)		
low signal peripheral high signal internal low signal	18(18.560%)	8(19.050%)	7(20.000%)	10.716②	0.098
peripheral low signal internal high signal equal signal	0(0.000%)	0(0.000%)	0(0.000%)		
	1(1.030%)	0(0.000%)	0(0.000%)		
	0(0.000%)	0(0.000%)	0(0.000%)		
MVI status					
Positive	66(68.040%)	27(64.290%)	17(48.570%)	4.220②	0.121
	31(31.960%)	15(35.710%)	18(51.430%)		

Categorical variables are expressed as frequency with percentages in parentheses. Qualitative variables are analyzed using Pearson's χ2 test or Fisher's exact test as appropriate, and quantitative variables are analyzed using the independent Samples t-test.P ; Traning cohort vs Internal testing cohort vs External testing cohort.T2WI T2-weighted, DWI diffusion-weighted imaging.

[a]Data are mean ± standard deviation

Table 2 Univariate analyses for preoperative microvascular invasion prediction in the training cohort

Variable	Univariate analysis		
	Odds ratio	(95% CI)	*P*
Age (year)	3.273	1.551-6.905	0.001*
Sex	0.721	0.306-1.701	0.458
Lesion Location	0.369	0.512-1.421	0.544
Tumor margin	1.931	0.942-3.959	0.072
T2WI tumor boundary	1.645	0.791-3.421	0.183
Bile duct dilatation	1.000	0.487-2.052	/
Hepatic capsule retraction	1.433	0.693-2.961	0.334
Intrahepatic bile duct stones	1.517	0.153-15.000	0.722
Vascular involvement	1.740	0.797-3.800	0.165
Vascular traversal Sign	2.014	0.887-4.572	0.092
Suspicious lymph nodes	1.995	0.690-5.767	0.199
T2WI signal Pattern	0.619	0.465-0.822	<0.001*
DWI signal Pattern	0.504	0.299-0.850	0.007*

Sex, DWI diffusionweighted imaging and T2WI T2-weighted imaging * $p < 0.05$

Radiomics characteristics

A total of 1590 features are extracted from the VOI of each sequence image. These features were divided into the following categories: (1) first-order statisti cal features are used to describe the distribution of pixel intensity, including m ean, median, standard deviation, skewness, and kurtosis; (2) shape features, whi ch are the geometric shapes of the tumor VOI, were quantified including volu me, surface area, compactness, and sphericity, and (3) texture features including gray level co-occurrence matrix (GLCM), gray level run length matrix (GLRL M), gray level size zone matrix (GLSZM), neighboring gray tone difference m atrix (NGTDM), and gray level dependence matrix (GLDM). These are used to describe the spatial relationships and provide structural information on the gray distribution in the image. The LASSO regression algorithm and MRMR algorit hm are used for feature selection. Finally, nine features were selected including two first-order statistical features, two gray level co-occurrence matrix features, one gray level run length matrix feature, three gray level region size matrix fe atures, and one gray level dependence matrix feature. The final features are sh own in Fig.3.

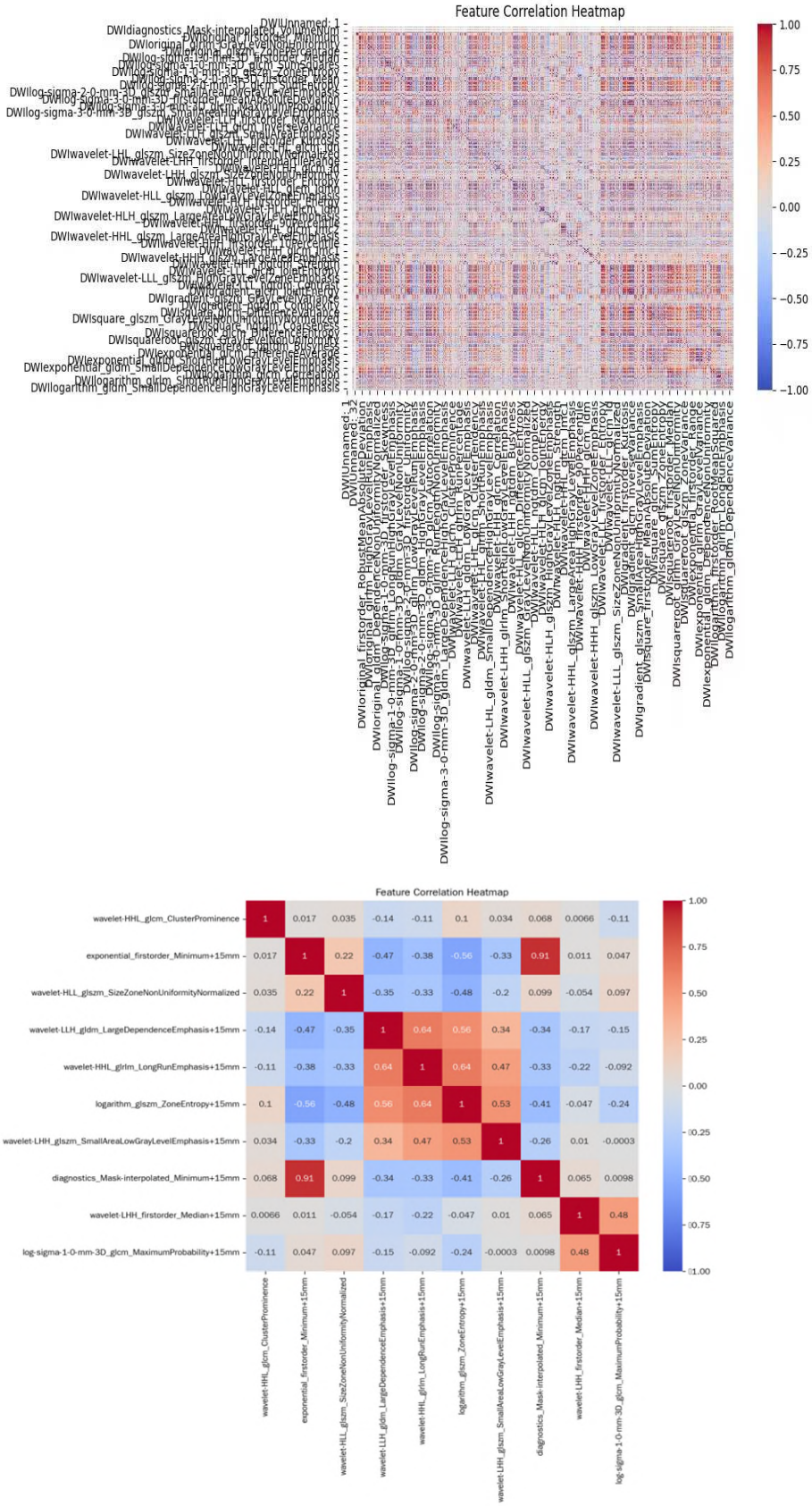


Figure 3 | Heatmaps of the features are extracted from the $VOI_{peri+15mm}$ of DWI.(a)All features.(b)The final features.

Radiomics model

As shown in Table S2, we evaluated a total of 72 MRI radiomics models based on different classifiers and different VOIs in the training cohort. Comparison of the different parameters identified the Random Forest classifier as the most effective model. The different VOIs of different sequences of the Random Forest classifier were used to select six models with different VOIs (Table 3). The predictive performance of the models was compared using the DeLong test. The model based on intratumoral + peritumoral 15 mm in DWI showed the highest predictive performance(Fig.4). The AUC of the model in the training cohort reached 0.984 [95% confidence interval (CI): 0.960-0.998]. The AUC values in the

test cohort and the external test cohort were 0.826 (95% CI: 0.696-0.941) and 0.735 (95% CI: 0.385-1.000), respectively(Fig.5).

Table 3-1 The comparison of various models in training cohort.

Trating cohort	Indexes					
	AUC（95%IC）	ACC	SEN	SPE	PPV	NPV
0 mm DWI	0.989（0.975-0.999）	0.952	0.967	0.913	0.967	0.913
0+3 mm DWI+T2WI	0.996（0.989-1.000）	0.964	1.000	0.842	0.955	1.000
0+5 mm DWI	0.996（0.987-1.000）	0.976	1.000	0.913	0.968	1.000
0+10 mm DWI	0.991（0.977-1.000）	0.964	1.000	0.870	0.952	1.000
0+15 mm DWI	0.984（0.960-0.998）	0.940	0.950	0.913	0.966	0.875
0+20 mm DWI+T2WI	0.989（0.971-0.999）	0.952	0.969	0.895	0.969	0.895

Table 3-2 The comparison of various models in Internal testing cohort.

Internal testing cohort	Indexes					
	AUC（95%IC）	ACC	SEN	SPE	PPV	NPV
0 mm DWI	0.625（0.404-0.817）	0.667	0.875	0.250	0.700	0.500
0+3 mm DWI+T2WI	0.763（0.537-0.936）	0.806	0.893	0.500	0.862	0.571
0+5 mm DWI	0.677（0.473-0.852）	0.722	0.875	0.417	0.750	0.625
0+10 mm DWI	0.785（0.614-0.944）	0.806	0.958	0.500	0.793	0.857
0+15 mm DWI	0.826（0.696-0.941）	0.778	0.875	0.583	0.808	0.700
0+20 mm DWI+T2WI	0.781（0.613-0.913）	0.750	0.893	0.250	0.806	0.400

CI confidence intervals, AUC area under the receiver operating characteristic curve

Model evaluation

The radiomics model showed the highest discriminative performance among all models (Fig.5). The AUC values of the combined model with clinical imaging factors were 0.991(95% CI: 0.970-1.000), 0.717(95% CI: 0.325-0.756), and 0.719 (95% CI: 0.367-1.000), respectively. The AUC of the internal test cohort was lower than that of the radiomics model. The training cohort and the external test cohort showed that the prediction efficiency of the combined model was slightly higher than that of the simple radiomics model(Table 4). The DeLong test results showed that the performance of the radiomics model was better than that ofthe clinical-imaging model and the combined model.

The calibration curve (Fig.5) shows that the prediction results of the radiomics models are in good agreement with the real results, indicating that the radiomics model showed superior predictive ability in the training cohort, internal test cohort, and external validation cohort. The DCA results (Fig.5) showed that theAUC of the radiomics model in the training cohort, internal test cohort, and external validation cohort was higher than that of the clinical-imaging model and the combined model, indicating that the radiomics model had a higher clinical net benefit than other models for predicting IMCC MVI.

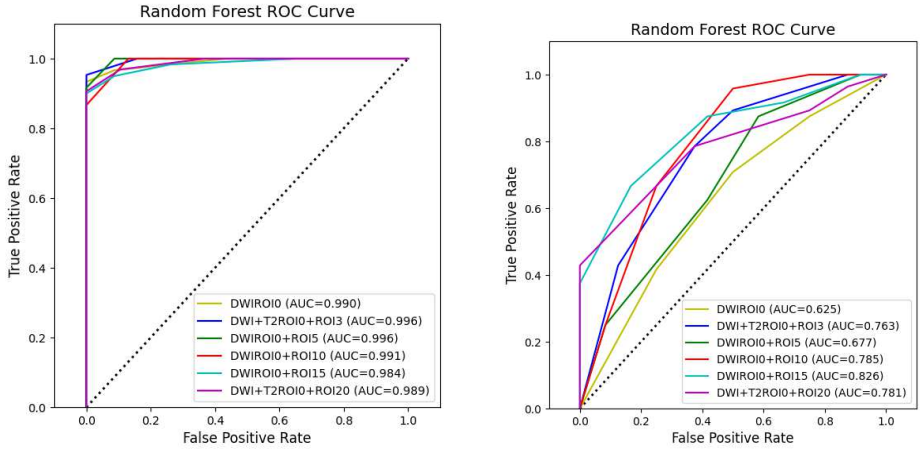


Figure 4 | The receiver operating characteristic curves of the six different VOIs in the training cohort(a) and internal validation cohort(b).AUC, area under the curve.

Table 4 The performance of MVI prediction models in training cohort and testing cohorts.

Indexes		AUC(95%CI)	ACC	SEN	SPE	PPV	NPV
Clinical Model	Internal tranting	0.813（0.716-0.901）	0.760	0.800	0.677	0.839	0.618
	Internal testing	0.819（0.655-0.953）	0.762	0.889	0.533	0.774	0.727
	External testing	0.663（0.309-1.000）	0.714	0.882	0.556	0.652	0.833
Radiomics Model	Internal tranting	0.984（0.959-0.998）	0.940	0.950	0.913	0.966	0.875
	Internal testing	0.826（0.696-0.941）	0.778	0.875	0.583	0.808	0.700
	External testing	0.735（0.381-1.000）	0.742	0.647	0.833	0.786	0.714
Combined Model	Internal tranting	0.991（0.970-1.000）	0.955	0.957	0.952	0.978	0.909
	Internal testing	0.717（0.325-0.756）	0.633	0.737	0.455	0.700	0.500
	External testing	0.719（0.367-1.000）	0.714	0.647	0.778	0.733	0.700

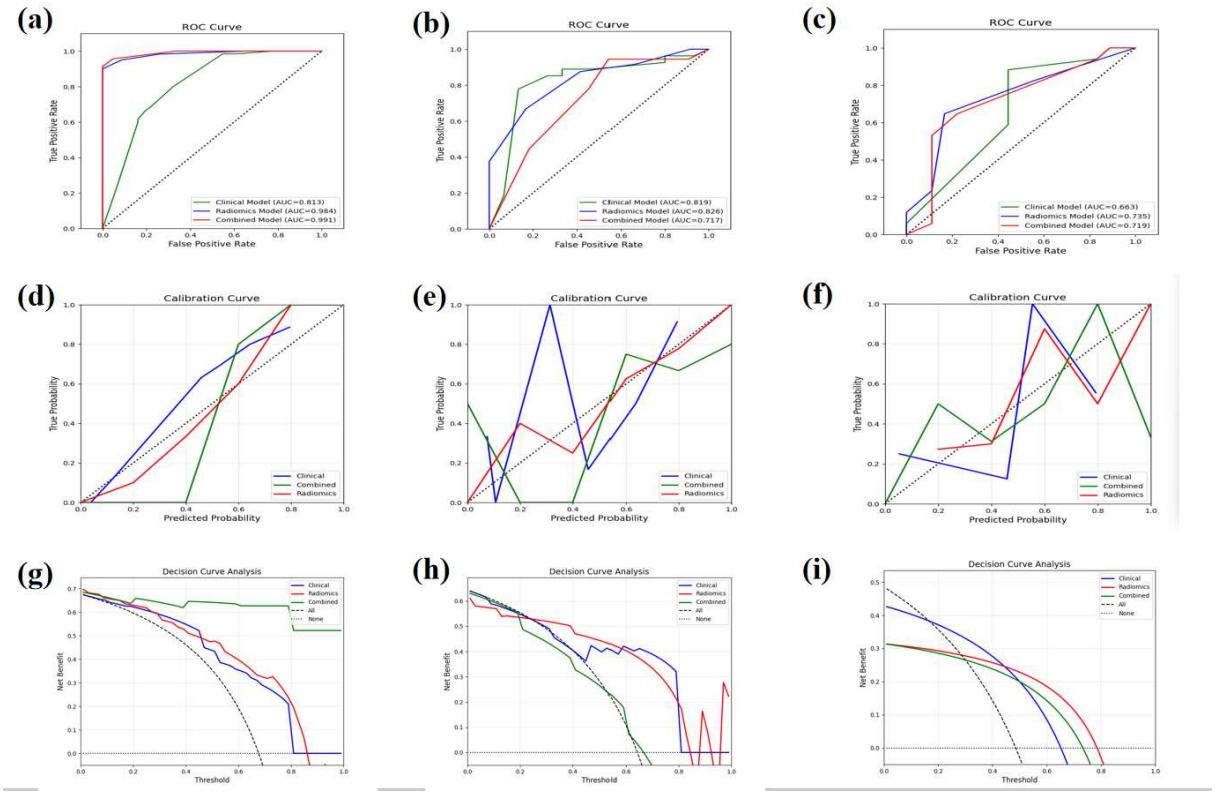


Figure 5 | The receiver operating characteristic curves (a–c), calibration curves (d–f), and decision curves (g–i) of the different models in the training cohort, internal validation cohort and external validation cohort.

Discussion

Radiomics model and clinical imaging model analysis

In this study, a radiomics model based on MRI sequences was established to predict the MVI status of IMCC patients before surgery. The final MVI predict ion model, which showed satisfactory performance, integrated radiomics features based on the DWI sequence intratumoral + peritumoral 15 mm with conventio nalimaging features such as gender, DWI signal intensity, and T2WI signal inte nsity.

In this study, four classifiers (Random Forest, Logistic Regression, XGBoost, and Gaussian Naive Bayes) were used to establish the radiomics model. Comparison of the parameters identified the Random Forest model as the most stable and the most effective in each VOI. Previous studies comparing different model construction methods reported that the Random Forest classification methodshows the highest prognostic performance[20,21]. This study further confirms the excellent performance of the Random Forest model for predicting IMCC MVI status.

The DWI sequence is mainly used to evaluate the diffusion of water molecules in tissues, and the microstructure of tissues can be visualized according to the degree of diffusion of water molecules. Zhang et al.[22] and Liu et al.[23] establi shed models based on DWI sequences to study IMCC and achieved good predictive results. Compared with multiple sequence models in this study, the DWI sequence model showed the best performance in predicting IMCC MVI status. Chen et al.[24] reported that the DWI-based nomogram showed better performance in predicting MVI (the AUC of the training cohort was 0.806) than other sequence radiomics models and clinical-imaging models.

In this study, we radially extended the distance from the tumor boundary to 3, 5, 10, 15, and 20 mm and delineated the tumor and five ranges of intratumora l and peritumoral tissues on the three sequences of T2WI, and DWI, yielding a total of six VOIs. Subsequently, single-sequence and double-sequence radiomi cs models were established for the six VOIs. In the intratumoral and intratumo ral+peritumoral 20 mm radiomics models, the DWI + T2WI dual-sequence radiomics model showed the highest predictive efficiency, whereas the other four VOIs were all DWI sequence models with the best performance; therefore, this study finally included six different VOI best models for comparison: dual-s equence intratumoral model, DWI sequence intratumoral + peritumoral 3 mm, DWI intratumoral + peritumoral 5 mm, DWI intratumoral + peritumoral 10 m m, DWI intratumoral + peritumoral 15 mm, and dual-sequence intratumoral + peritumoral20 mm.The results showed that in all radiomics models, the intratu moral+peritumoral model showed superior predictive performance, which was hi gher than
that of the intratumoral model. A larger range yielded a higher predictive performance, confirming that MVI usually appears in the peritumoral area. Extr acting radiomics features from the peritumoral area has important clinical signif icance forpredicting tumor MVI[17]. Previous studies found that the intratumoral and peritumoral 10 mm extraction model is superior to the intratumoral model and other range models[25,26]. However, the previous study did not include the

tumor's range at 15 mm; therefore, this study has a different reference value. Multiple MRI radiomics models identified preoperative carbohydrate antigen 19-9 (CA19-9) level, tumor size, intrahepatic duct dilatation, multiple tumors, tumor margin, tumor morphology, peritumoral high signal, arterial phase enhancement mode, and apparent diffusion coefficient as independent predictors of ICC MVI[27-30]. Because the predictors differ among models, the predictive value of the above predictors for MVI status in ICC patients is not clear. In this study, gender, age, and conventional radiological features were included to establish a clinical imaging model. After univariate logistic analysis, gender, T2WI signal intensity and DWI signal intensity were included to establish a model, which showed good predictive efficacy.

Different signal characteristics of tumors on T2WI and DWI images were included in the study, and the analysis included whether the signal intensity was uniform and whether there was a target sign. Finally, it was identified as an independent predictor of IMCC MVI. In the training cohort, imaging features showed stronger predictive value. Among them, T2WI signal uniformity ($p = 0.006$) and DWI performance ($p = 0.010$) were significantly correlated with MVI status. The MVI-positive group showed a trend towards an 'uneven high signal'. Histologically, ICC often presents with aggressive characteristics, and inflammation, necrosis, and fibrosis are common[31]. Therefore,the heterogeneity of signal intensity in MRI images is more significant in MVI-positive ICC, which is consistent with the first-order homogeneity feature[32].

This study found that the radiomics features of intratumoral + peritumoral 15 mm from the DWI sequence had the best predictive value, including two first-order statistical features and seven texture features, of which six features were based on filtering processing. We found that the texture features wavelet-HHL_glrlm_Long Run Emphasis and wavelet-LLH_gldm_Large Dependence Emphasis after wavelet transform were strongly positively correlated with MVI. A study on early screening of pulmonary nodules found that wavelet transform increases the information provided by low-frequency signals and extracts deeper, high-throughput features that are invisible to the naked eye[33]. These studies confirm that filtered radiomics features can extract multi-scale and multi-directional image information and better reflect tumor heterogeneity.

Combined model analysis

Finally, a combined model was established by combining the radiomics features of the intratumoral + peritumoral 15 mm model based on DWI sequencewith gender, T2WI signal features, and DWI signal features. This model showed predictive efficacy, but it was slightly lower than that of the simple radiomics model, demonstrating that clinical imaging factors did not improve the predictiveefficacy of the radiomics model for IMCC MVI. In the future, additional clinicalfeatures such as tumor markers and TNM staging will be included to establish a multimodal combined model to predict the MVI status of IMCC patients.

This study was a multi-center study, and two different medical institutions were included for external validation; the model was established using six different

VOI extraction features. In all three, the simple radiomics model, clinical imaging model, and combined model, the AUC values were higher than 0.6, confirming the effectiveness of the model.

Limitations

(1) This study was a multi-center retrospective study, and selection bias cannotb e ruled out. In addition, the data sources differed regarding the equipment (2) and parameters, and the images have certain heterogeneity. (2) The sample size was small, and additional data will be collected in the future to determine the generalizability of the model. (3) In this study, most cases were examined by MRI within 4 weeks or even 1 week before biopsy; however, there were a few cases examined at more than 4 weeks. The follow-up study should strictly control the time interval. (4) This study did not include clinical features such astumor markers. Future studies will include additional features to establish clin ical-imaging models and to increase the effectiveness of the model.

Conclusion

In summary, MRI-based intratumoral and peritumoral radiomics features can eff ectively predict IMCC MVI before surgery. The intratumoral + peritumoral 15 mm based on DWI sequence was the most effective radiomics model. Its appli cation will help clinicians design personalized treatment plans and follow-up plans, which is important for evaluating the prognosis of patients.

References:

[1] Massarweh NN, El-Serag HB（2017）Epidemiology of hepatocellular carcin oma and intrahepatic cholangiocarcinoma. *Cancer Control* 24: 107327481772924 5.

[2] Cerrito L, Ainora M E, Borriello R, et al（2023）Contrast-enhanced imagin g in the management of intrahepatic cholangiocarcinoma: state of art and future perspectives. *Cancers* 15(13): 3393

[3] European Association for the study of the liver（2023）EASL-ILCA Clinica l Practice Guidelines on the management of intrahepatic cholangiocarcinoma. *J Hepatol* 79(1): 181-208

[4] Lim J H（2003）Cholangiocarcinoma: morphologic classification according t o growth pattern and imaging findings. *AJR Am J Roentgenol* 181(3):819-27[5] Mazzaferro V, Gorgen A, Roayaie S, et al（2020）Liver resection and transpl antation for intrahepatic cholangiocarcinoma. *J Hepatol* 72(2): 364-377

[6] Rodriguez-Perálvarez M, Luong TV, Andreana L, et al（2013）A systematic reviewof microvasculalinvasion in hepatocellular carcinoma: diagnostic and prog nostic variability. *Ann SurgOncol* 20(1): 325-339

[7] Chen Y F, Liu H Z, Zhang J Y, et al（2021）Prognostic value and predicat ion model of microvascular invasion in patients with intrahepatic cholangiocarci noma:a multicenter study from China. *BMC Cancer* 21(1): 1299

[8] Maki H, Kawaguchi Y, Nagata R, et al(2023) Conditional recurrence analys is of intrahepatic cholangiocarcinoma: changes in recurrence rate and survivalaft er recurrence resection by disease-free interval. Hepatol Res 53(12): 1224-1234

[9] Sun Z Q, Han X, You W L, et al(2023) Adjuvant therapy for cholangiocar

cinoma after surgery and prognosis factors for cholangiocarcinoma: a single-cen ter retrospective cohort study. *Front Oncol* 13: 1116338
[10] Xu Y, Li Z, Zhou Y Z, et al(2023) Using immunovascular characteristics t o predict very early recurrence and prognosis of resectable intrahepatic cholangi ocarcinoma, *BMC Cancer* 23(1): 1009
[11] European Association for the Study of the Liver(2023) EASL-ILCA Clinica l Practice Guide lines on the management of intrahepatic cholangiocarcinoma. *J Hepatol* 79(1): 181–208
[12] Gillies R J, Kinahan P E, Hricak H(2016). RadiRadiomics: images are mo re than pictures, they are data. *Radiology* 278(2): 563-577
[13] Liu Z Y, Wang S, Dong D, et al(2019), The applications of Radiomicsin precision diagnosis and treatment of oncology: opportunities and challenges [J]. Theranostics 9(5): 1303-1322
[14] Guiot J, Vaidyanathan A, Deprez L, et al(2022). A review in radiRadiomi cs: making personalized medicine a reality via routine imaging. *Med Res Rev* 42(1): 426-440
[15] Zhou Y, Zhou G F, Zhang J L, et al(2021). Radiomicssignature on dynami c contrast-enhanced MR images: a potential imaging biomarker for prediction o f microvascular invasion in mass-forming intrahepatic cholangiocarcinoma. Eur Radiol 31(9): 6846-6855
[16] Tang Z, Liu W R, Zhou P Y, et al(2019) Prognostic value and predication model of microvascular invasion in patients with intrahepatic cholangiocarcino ma. *J Cancer* 10(22): 5575-5584
[17] Silva M, Vivancos C, Duffau H(2022) The concept of «Peritumoral zone» in diffuse low-grade gliomas: oncological and functional implications for a con nectome-guided therapeutic attitude. *Brain Sci* 12(4): 504
[18] Choi SY, Kim YK, Min JH, et al(2018) Added value of ancillary imaging features for differentiating scirrhous hepatocellular carcinoma from intrahepatic cholangiocarcinoma on gadoxetic acid-enhanced MR imaging. *Eur Radiol* 28 (6):2549-2560
[19]Lewis S, Besa C, Wagner M, et al(2018) Prediction of the histopathologic findings of intrahepatic cholangiocarcinoma: qualitative and quantitative assessm ent ofdiffusion-weighted imaging. *Eur Radiol* 28(5):2047-2057
[20] Zhang Y, Oikonomou A, Wong A, et al(2017) RadiRadiomics-based progn osis analysis for non-small cell lung cancer. *Sci Rep* 7: 46349
[21] Parmar C, Grossmann P, Bussink J, et al(2015) Machine learning methods for quantitative radiomic biomarkers. *Sci Rep* 5: 13087
[22] Zhang Y F, Chen J J, Yang C, et al(2024) Preoperative prediction of micr ovascular invasion in hepatocellular carcinoma using diffusion-weighted imaging -based habitat imaging.*Eur Radiol* 34(5): 3215-3225
[23] Liu Y L, Wang B, Mo X, et al(2022) A deep learning workflow for mass -forming intrahepatic cholangiocarcinoma and hepatocellular carcinoma classifica tion based on MRI. *Curr Oncol* 30(1): 529-544
[24] Chen S, Zhu Y, Wan L, et al(2023) Predicting the microvascular invasion

and tumor grading of intrahepatic mass-forming cholangiocarcinoma based on magnetic resonance imaging Radiomicsand morphological features. *Quant Imaging Med Surg* 13(12):8079-8093
[25] Wang Q, Qian X, Zhang Y, et al(2025) Multi-regional Radiomicsfor predicting microvascular invasion and lymph node metastasis in intrahepatic cholangiocarcinoma. *Clin Radiol* 88: 106979
[26] Ma X, Qian X, Wang Q, et al(2023) Radiomicsnomogram based on optimal VOI of multi-sequence MRI for predicting microvascular invasion in intrahepaticcholangiocarcinoma. *Radiol Med* 128(11): 1296-1309
[27] Ma X J, Liu L H, Fang J, et al(2020) MRI features predict microvascular invasion in intrahepatic cholangiocarcinoma. *Cancer Imaging* 20(1): 40
[28] Zhou Y, Wang X L, Xu C, et al(2019). Mass-forming intrahepatic cholangiocarcinoma: can diffusion-weighted imaging predict microvascular invasion? *J Magn Reson Imaging* 50(1): 315-324
[29] Chen S, Wan L J, Zhao R, et al(2023) Predictive factors of microvascular invasion in patients with intrahepatic mass-forming cholangiocarcinoma based on magnetic resonance images. *Abdom Radiol* 48(4): 1306-1319
[30] Sheng R, Zheng B, Zhang Y, et al(2025) MRI-based microvascular invasion prediction in mass-forming intrahepatic cholangiocarcinoma: survival and therapeutic benefit. *Eur Radiol* 35(7):4068-4079
[31] Sempoux C, Jibara G, Ward SC, et al(2011). Intrahepatic Cholangiocarcinoma: New Insights in Pathology. *Semin Liver Dis* 31:49–60
[32] Zhou Y, Zhou G F, Zhang J L, et al(2021). Radiomicssignature on dynamic contrast-enhanced MR images: a potential imaging biomarker for prediction of microvascular invasion in mass-forming intrahepatic cholangiocarcinoma. *Eur Radiol* 31(9): 6846-6855
[33] Jing R, Wang J, Li J, et al(2021) A wavelet features derived Radiomicsnomogram for prediction of malignant and benign early-stage lung nodules. *Sci Rep* 11(1):22330

Supplementary Files

This is a list of supplementary files associated with this preprint. Click to download.

- SupplementaryMaterial.docx